ELSEVIER

Free- and forced-convection film condensation from a horizontal elliptic tube with a vertical plate and horizontal tube as special cases

Sheng-An Yang and Chao-Ho Hsu
Department of Mould and Die Engineering, National Kaohsiung Institute of Technology, Kaohsiung, Taiwan, ROC

A simple mathematical model is developed for the study of the mixed-convection film condensation with downward flowing vapors onto a horizontal elliptic tube. Analytical analysis for both the local condensate film thickness and heat transfer characteristics under simultaneous effects of interfacial vapor shear and pressure gradient has been performed by adopting a unified geometry parameter, eccentricity e. The present results for two limit cases, $e=0$ (circular tube) and $e=1.0$ (vertical plate) are in an excellent agreement with the earlier works. For very slow vapor flow, the present result for dimensionless mean heat transfer coefficient reduces to the same form as in the earlier works, $\overline{Nu}(Ja/Ra)^{1/4}$, whose value is 0.728 for $e=0$ and 0.943 for $e=1.0$. As for very fast vapor flow, the dimensionless mean heat transfer coefficient, $\overline{Nu}\,Re^{-1/2}$ increase with increasing eccentricity under the effects of pressure gradient caused by potential flow and surface tension.

Keywords: film condensation; elliptic tube; mixed convection; surface tension

Introduction

Much effort has been directed toward predicting heat transfer by filmwise condensation from the external surfaces of bodies of various contours since the original work of Nusselt (1916). For free-convection film condensation on vertical plates and circular cylinders, the pioneering Nusselt theory has been found in later more complete studies, such as, Rohesnow (1956), Sparrow and Gregg (1959), and Churchill (1986), to be generally valid. For a circular tube and vertical plate, the mean condensing heat transfer coefficient can be calculated with good accuracy from: $\overline{Nu}=0.728\ (Ra/Ja)^{1/4}$ and $0.943\ (Ra/Ja)^{1/4}$ respectively. Yang and Chen (1993) employed *eccentricity* of ellipse to unify the various geometries from $e=0$ circular tube to $e=1.0$ vertical flat plate in investigating free-convection condensation heat transfer and obtained good results in agreement with the above limiting cases: $e=0$ and $e=1.0$. In view of Yang and Chen's work, the same approach using *eccentricity* to treat the forced-convection condensation heat transfer problem might be achieved.

As far as the forced-convection condensation is concerned, Shekriladze and Gomelauri (1966) obtained numerical solutions by utilizing the asymptotic shear stress at the interface, including the effects of gravity force and velocity of vapor, without accounting for the pressure gradient term around a circular tube. Afterward, based upon Shekriladze and Gomelauri's model, Rose (1984) took further account of the pressure gradient effect upon forced-convection film condensation on a horizontal circular tube with vertical vapor downflow using potential flow theory. Rose proposed a good empirical expression for mean Nusselt number and found that inclusion of the pressure gradient led to a small decrease in the mean heat-transfer coefficient. A better representation of vapor shear stress was made by Fujii et al. (1972), where solution of the two-phase liquid and vapor boundary-layer equations was made with matching of the shear stress at the interface. Their results do not differ greatly from that of Rose, except at low condensation rates.

All the above works consider forced-convection film condensation on a circular tube, while limited analysis has been conducted on tubes of noncircular cross section. An elliptic cylinder, with major axis aligned with the direction of gravity, has proved to provide more enhanced heat transfer rates than a circular cylinder with an equivalent condensing surface area, particularly in the free-convection film condensation (Karimi 1977; Yang and Chen 1993). For forced-convection film condensation of downward flowing vapor on a horizontal elliptic cylinder, Panday (1987) developed an explicit numerical method to treat two-phase boundary-layer equations, including convection and inertia term in the condensate film equations, as well as pressure gradient and surface tension. Panday also employed the Shekriladze and Gomelauri (1966) model for interfacial shear stress to approximate the condensation rate; however, several mistakes in the numerical results have been mentioned by Adams et al. (1993). Moreover, Panday's result is opposite to the earlier work, partic-

Address reprint requests to Prof. Sheng-An Yang, Department of Mould and Die Engineering, National Kaohsiung Institute of Technology, 415 Chian-Kung Road, Kaohsiung 807, Taiwan, ROC.

Received 21 September 1996; accepted 13 January 1997

Int. J. Heat and Fluid Flow 18: 567–574, 1997

655 Avenue of the Americas, New York, NY 10010

0142-727X/97/$17.00
PII S0142-727X(97)00025-8

ularly in the free-convection film condensation; i.e. the mean heat transfer coefficient should be increased with eccentricity of ellipse with major axis aligned with the direction of gravity.

Considerable progress has been made towards the theoretical development of condensation with inclusion of surface tension effect. According to Krupiczka (1985), the effect of surface tension caused by curvature of the condensate film in a simple Nusselt-type analysis on a circular cylinder can be ignored, except for a small diameter tubes or wires, where the rapidly changing film thickness cannot be considered insignificant compared to a circular cylinder of the same surface area. Yang and Chen (1993) also studied the effect of surface tension on an elliptic tube caused by curvature of the surface and concluded that surface tension had negligible effect for $e < 0.8$ on the mean heat transfer coefficient.

Although Adams et al. (1993) have investigated the free- and forced-convection laminar film condensation on a horizontal elliptic tube with inclusion of the surface tension effect, too, they still used the ratio of minor axis/major axis of ellipse as eccentricity as Panday (1987) did, which is not a real definition in mathematics. Thus, their value of eccentricity is infinity for a horizontal flat plate, which does not easily yield the limiting case —horizontal flat plate. The present study uses actual eccentricity from mathematics to investigate the same problem of Adams et al., and also investigates how the transition from the free-convection film condensation to forced-convection film condensation occurs. Moreover, the present mathematical model can easily be reduced to the two limiting cases: pure free-convection film condensation and forced-convection film condensation for a vertical flat plate and a circular tube, respectively. Compared to the work of Adams et al., the present work not only offers a simpler analytical approach but also shows how the critical angle of the condensate film affects the mean heat transfer coefficient. Furthermore, we can see the difference between the effect upon the mean heat transfer coefficient with respect to the critical angle ϕ_c profiles with and without the pressure gradient in the present work. The major aim here is to restudy the problem of Adams et al. and to extend the work of Yang and Chen's (1993) into the mixed-convection film condensation by Rose's (1984) model and *eccentricity* from mathematics. There is more discussion about the influence of the critical angle on the heat transfer performance and on the transition from forced-convection to free-convection film condensation as F (the ratio of free-convection to forced-convection) increases.

Analysis

Consider a horizontal elliptical tube, with its major axis "2a" oriented in the direction of gravity, immersed in a downward flowing, pure vapor that is at its saturation temperature T_{sat} and moves at uniform velocity U_∞. The uniform wall surface temperature T_w is below the saturation temperature. Thus, condensation occurs on the wall, and a continuous film of the liquid runs downward over the tube under the combined effects of gravity, pressure gradient forces, and the interfacial vapor shear forces.

Notation

a, b	semimajor, semiminor axis of ellipse
Bo	Bond number, $(\rho - \rho_v)ga^2/\sigma$
C_p	specific heat of condensate at constant pressure
D_e	equivalent diameter of elliptic tube
e	eccentricity of ellipse, $\sqrt{1-(b/a)^2}$
F	dimensionless parameter, $(\mathrm{Ra}/\mathrm{Ja})/\mathrm{Re}^2$
g	acceleration due to gravity
h	condensing heat transfer coefficient at angle ϕ
$\bar{h}$	mean value of condensing heat transfer coefficient
h_{fg}	latent heat of condensate
Ja	Jakob number, $Cp\,\Delta T/h'_{fg}$
k	thermal conductivity of condensate
l	length of flat plate
m''	condensate mass flux (per unit area)
Nu, $\overline{\mathrm{Nu}}$	local and mean Nusselt number, (hD_e/k) and $(\bar{h}D_e/k)$ for elliptic tube
$\overline{\mathrm{Nu}}_l$	mean Nusselt number $= (\bar{h}l/k)$ for flat plate
p	static pressure of condensate
P	the dimensionless pressure gradient parameter, $(\rho_v/\rho)\,\mathrm{Pr}/\mathrm{Ja}$
Pr	Prandtl number
r	radial distance from centroid of ellipse to tube wall
R	radius of elliptic surface curvature
Ra	Rayleigh number, $\rho(\rho - \rho_v)g\ \mathrm{Pr}\ D_e^3/\mu^2$
Re	two-phase mean Reynolds number, $(\rho D_e U_\infty/\mu)$
Re_l	two-phase Reynolds number for flat plate, $\rho U_\infty l/\mu$
T_{sat}	saturation temperature of vapor
T_w	wall temperature
u_e	the tangential vapor velocity at the edge of the boundary layer
U_∞	the vapour velocity of the main free stream
u	velocity component in x-direction
x	coordinate measuring distance along circumference from top of tube
y	coordinate normal to the elliptic surface

Greek

δ	local thickness of condensate film
δ^*	dimensionless thickness of condensate film
θ	angle measuring from top of tube
μ	absolute viscosity of condensate
ρ	density of condensate
ρ_v	density of vapor
σ	surface tension coefficient in the film
ϕ	the angle between the tangent to tube surface and the normal to direction of gravity
τ_δ	the interfacial vapor shear stress

Subscripts

c	critical condition
sat	saturation
v	vapor
w	tube wall

Superscripts

*	dimensionless
–	averaged

(*Note*: when not subscripted, a property is taken as that of the liquid phase.)

The physical model under consideration is shown in Figure 1. The conservation of mass, momentum, and energy for the steady laminar layer flow are described by the following equations:

$$m'' = \rho \frac{\mathrm{d}}{\mathrm{d}x}\int_0^{\delta} u\,\mathrm{d}y \tag{1}$$

$$\mu\frac{\partial^2 u}{\partial y^2} + (\rho - \rho_v)g\sin\phi - \frac{\mathrm{d}p}{\mathrm{d}x} = 0 \tag{2}$$

$$h'_{fg}m'' = k\frac{\partial T}{\partial y} = k\frac{\Delta T}{\delta} \tag{3}$$

where $h'_{fg} = h_{fg} + 3Cp\,\Delta T/8$ is the latent heat of condensation corrected for condensate subcooling by Rohsenow (1956), and $\phi = \phi(x)$ is the angle between the normal to gravity and the tangent to the tube wall at the position (r, θ).

The conservation of mass is given in integral form by Equation 1. The momentum equation, Equation 2, reflects a balance of viscous, gravitational, and pressure gradient effects through the first, second, and third terms, respectively. The energy equation, Equation 3, is a balance between the latent heat released at the interface through condensation, and heat flux conducted through the condensate film to the elliptic wall surface.

Introducing a parameter, $e = \sqrt{a^2 - b^2}/a$, the eccentricity of the ellipse, then we can express an equivalent diameter D_e, based on the same condensing surface area as follows:

$$D_e = 2\frac{a}{\pi}\int_0^{\pi}\left[(1-e^2)\Big/\sqrt{(1-e^2\sin^2\phi)^3}\right]\mathrm{d}\phi \tag{4}$$

As seen in the earlier study of Yang and Chen (1993), we can derive the differential streamwise length in terms of D_e and e in the following relationship:

$$\mathrm{d}x = D_e I_f(\phi)\,\mathrm{d}\phi/2 \tag{5}$$

where

$$I_f(\phi) = \left[\pi\Big/\sqrt{(1-e^2\sin^2\phi)^3}\right]\Big/\int_0^{\pi} 1\Big/\sqrt{(1-e^2\sin^2\phi)^3}\,\mathrm{d}\phi \tag{6}$$

Because of the very thin film thickness, compared with the radius of surface curvature, we can approximately express the pressure gradient along the interface to be a combination of that caused by potential flow and surface tension as follows:

$$\frac{\mathrm{d}p}{\mathrm{d}x} = -\rho_v u_e\frac{\mathrm{d}u_e}{\mathrm{d}x} - \frac{\sigma}{R^2}\frac{\partial R}{\partial x} \tag{7}$$

where R, the radius of curvature of the ellipse at the position (r, θ), can be derived as

$$R = \left(a\Big/\sqrt{1-e^2}\right)[(1+e^2(e^2-2)\cos^2\theta)/(1-e^2\cos^2\theta)]^{3/2} \tag{8}$$

Thus, inserting Equation 7 into Equation 2 yields

$$\mu\frac{\partial^2 u}{\partial y^2} = -(\rho - \rho_v)\,g\sin\phi - \frac{\sigma}{R^2}\frac{\partial R}{\partial x} - \rho_v u_e\frac{\mathrm{d}u_e}{\mathrm{d}x} \tag{9}$$

subjected to the following boundary conditions:

$$\frac{\partial u}{\partial y} = \tau_\delta/\mu, \qquad \text{at} \qquad y = \delta \tag{10}$$

and

$$u = 0, \qquad \text{at} \qquad y = 0 \tag{11}$$

Here, the interfacial vapor shear, Equation 10, should be modeled. This could be carried out by numerical approach to the two-phase conservation equations; however, the usefulness and simplicity of the present study would probably be violated through such an approach, as mentioned in Jacobi (1992). A good approximation for high condensation rates is given by Shekriladze and Gomelauri's (1966) model as

$$\tau_\delta = m'' u_e \tag{12}$$

The above approximation has limitations, and another model of Blangetti and Naushahi (1980) may be used; however, Equation 12 is useful in its simplicity and is also employed in Jacobi (1992) to yield good results.

According to potential flow theory, for a uniform flow with velocity U_∞ past an elliptic tube, we can derive the vapor velocity at the edge of boundary layer as

$$u_e = U_\infty(1 + \sqrt{1-e^2})\sin\phi \tag{13}$$

and thence obtain the pressure gradient due to the potential flow by using Equation 5

$$\rho_v u_e\frac{\mathrm{d}u_e}{\mathrm{d}x} = \rho_v U_\infty^2(1+\sqrt{1-e^2})^2\sin 2\phi/D_e I_f(\phi) \tag{14}$$

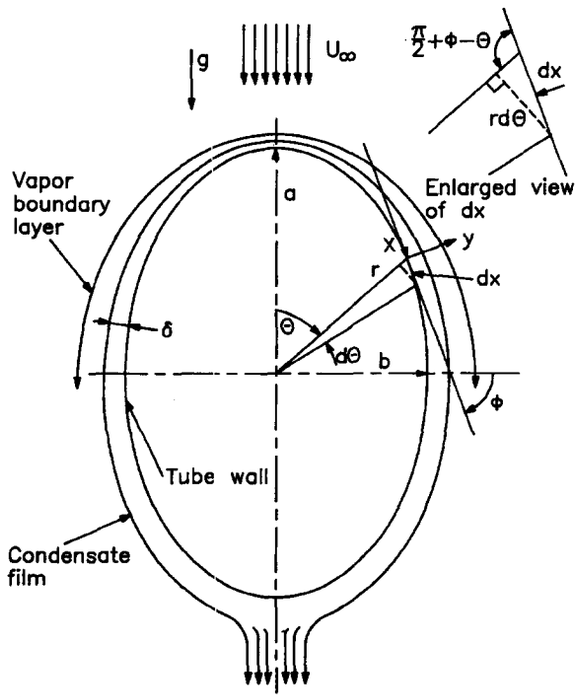

Figure 1 Physical model and coordinate system

Furthermore, as derived in Yang and Chen (1993), the pressure gradient due to the surface tension is written as follows:

$$\frac{\sigma}{R^2}\frac{\partial R}{\partial x} = (\rho - \rho_v)\, g\, \mathrm{Bo}(\phi) \tag{15}$$

where

$$\mathrm{Bo}(\phi) = \frac{3e^2}{2\,\mathrm{Bo}}\left(\frac{1-e^2\sin^2\phi}{1-e^2}\right)^2 \sin 2\phi,$$

and Bond number

$$\mathrm{Bo} = (\rho - \rho_v) g a^2/\sigma.$$

Consequently, by substituting the Equations 14 and 15 into Equation 7, the resultant momentum equation can be solved as follows:

$$u = m'' U_\infty (1+\sqrt{1-e^2})\, y \sin\phi/\mu + \left\{(\rho-\rho_v)\, g\,[\sin\phi + \mathrm{Bo}(\phi)] + \rho_v U_\infty^2 (1+\sqrt{1-e^2})^2 \sin 2\phi / D_e I_f(\phi)\right\}\left(y\delta - \frac{1}{2}y^2\right)\Big/\mu \tag{16}$$

Inserting Equation 3 into Equations 1 and 10 to eliminate m'', and integrating the updating Equation 1 by using Equation 16, and then introducing dimensionless parameters yield

$$\frac{2\delta^*}{I_f(\phi)}\frac{\mathrm{d}}{\mathrm{d}\phi}\left\{\delta^*\frac{1+\sqrt{1-e^2}}{2}\sin\phi + \frac{1}{3}\delta^{*3}F[\sin\phi + \mathrm{Bo}(\phi)] + \frac{\delta^{*3}}{3}P(1+\sqrt{1-e^2})^2 \sin 2\phi / I_f(\phi)\right\} = 1 \tag{17}$$

with the boundary condition:

$$\mathrm{d}\delta^*/\mathrm{d}\phi = 0 \qquad \text{at } \phi = 0 \tag{18}$$

where,

$$\delta^* = (\delta/D_e)\sqrt{\mathrm{Re}}\,; \quad F = (\mathrm{Ra}/\mathrm{Ja})/\mathrm{Re}^2; \quad P = (\rho_v/\rho)\,\mathrm{Pr}/\mathrm{Ja} \tag{19}$$

The first term inside the derivative in Equation 17 results from the interfacial shear stress, while the term involving P is the effect of pressure gradient due to the potential flow. When both of these terms are omitted, Equation 17 reduces to the pure free-convection film condensation, which was investigated by Yang and Chen (1993).

Applying the boundary condition, Equation 18 into Equation 17, we can obtain the expression for the condensate film thickness at $\phi = 0$, δ_0^*, as

$$I_f(0)/(2\delta_0^*) - \delta_0^*\frac{1+\sqrt{1-e^2}}{2} - \frac{1}{3}\left\{F\left[1 + 3e^2\left(\frac{1}{1-e^2}\right)^2\Big/\mathrm{Bo}\right] + \frac{2P}{I_f(0)}(1+\sqrt{1-e^2})^2\right\}\delta_0^{*3} = 0 \tag{20}$$

Note that above nonlinear equation can be solved for the condensate film thickness at $\phi = 0$, δ_0^* by using the Newton–Raphson iteration method.

Before proceeding to solve Equation 17, and thence to calculate the heat transfer rate for the elliptic tube, it should be noted that the condensate film flow may happen to separation when the following condition exists:

$$(\partial u/\partial y)_{y=0} \le 0 \tag{21}$$

Thus, this condition may also be obtained by Equation 17 in the following relationship:

$$\frac{1+\sqrt{1-e^2}}{2} + \left\{F[1 + \mathrm{Bo}(\phi)/\sin\phi] + 2P(1+\sqrt{1-e^2})^2 \cos\phi / I_f(\phi)\right\}\delta^{*2} = 0 \tag{22}$$

If $\phi = \phi_c$ satisfies the above equation, ϕ_c is called the critical angle; i.e.,

$$\mathrm{d}\delta^*/\mathrm{d}\phi \to \infty \qquad \text{as} \qquad \phi \to \phi_c \tag{23}$$

However, because δ^* is unknown, it should be solved by means of a fourth-order Runge–Kutta integration. Next, substituting δ^* into Equation 22 and employing a Bisection method will give the position or value of ϕ_c. By the way, it is very unstable and sensitive to calculate δ^* at ϕ close to ϕ_c, so we are required to check if the condensate film thickness will abruptly become extra thick; i.e.

$$\delta^* \to \infty \qquad \text{as} \qquad \phi \to \phi_c \tag{24}$$

Obviously, when

$$F \ge \frac{2P}{\pi}(1+\sqrt{1-e^2})^2 \int_0^\pi (1-e^2\sin^2\phi)^{-3/2}\mathrm{d}\phi \tag{25}$$

it satisfies, $\phi_c = \pi$. These cases mean that the condensate film will separate or drip off at the bottom of the tube. Otherwise,

$$F < \frac{2P}{\pi}(1+\sqrt{1-e^2})^2 \int_0^\pi (1-e^2\sin^2\phi)^{-3/2}\,\mathrm{d}\phi \tag{26}$$

the critical angle becomes, $\pi/2 < \phi_c \le \pi$. These cases indicate that the condensate film will drip off before reaching the bottom of the tube. Because for the latter cases, solutions will not be possible beyond ϕ_c, we can ignore the contribution to heat transfer from extra large film thickness. Note that, for $e = 0$, Equations 25 and 26 reduce to that given by Rose (1984) for a circular tube.

As in Nusselt's theory, the dimensionless local heat transfer coefficient at a particular angle ϕ may be expressed as

$$\mathrm{Nu} = \frac{D_e}{\delta} = \sqrt{\mathrm{Re}}\,/\delta^* \tag{27}$$

Next, we are interested in an expression for the overall mean heat transfer coefficient. Integrating Equation 27 over a whole tube, but neglecting the contribution to the heat transfer beyond ϕ_c based on the whole surface area gives

$$\overline{\mathrm{Nu}}\,\mathrm{Re}^{-1/2} = \int_0^{\phi_c}[I_f(\phi)/\delta^*]\,\mathrm{d}\phi \Big/ \int_0^{\pi} I_f(\phi)\,\mathrm{d}\phi$$

$$= \int_0^{\phi_c}\left[(1-e^2\sin^2\phi)^{-3/2}/\delta^*\right]\mathrm{d}\phi \Big/$$

$$\int_0^{\pi}(1-e^2\sin^2\phi)^{-3/2}\,\mathrm{d}\phi \qquad (28)$$

For $e = 1$, it is noted that an elliptic tube becomes a vertical flat plate with condensation at both sides occurring. Thus, its equivalent diameter D_e equals $2l/\pi$. Here, l is a characteristic length of the vertical plate. Therefore, we should use l instead of D_e for Re and $\overline{\mathrm{Nu}}$ in Equation 28 as follows:

$$\overline{\mathrm{Nu}}_l\mathrm{Re}_l^{-1/2} = \int_0^{l}(1/\delta^*)\,\mathrm{d}x/l \qquad (29)$$

It should be noted that, at low vapor velocity, Equation 28 blends with the Nusselt-type solution. Furthermore, there are two asymptotic cases explained as follows.

Firstly, for the cases where $F \gg 1$; i.e., for very slow vapor flow, the gravity force is much larger than vapor shear force and the pressure gradient attributable to the potential flow. Hence, the problem reduces to the free-convection film condensation; i.e., Yang and Chen's (1993) study. After omitting the first term and final term in Equation 17, we have

$$\frac{2\delta^*}{I_f(\phi)}\frac{\mathrm{d}}{\mathrm{d}\phi}\left\{\frac{1}{3}\delta^{*3}F[\sin\phi + \mathrm{Bo}(\phi)]\right\} = 1 \qquad (30)$$

By using the separation of variables, we can obtain

$$\delta^* = F^{-1/4}[\sin\phi + \mathrm{Bo}(\phi)]^{-1/3}$$

$$\times\left[2\int_0^{\phi} I_f(\phi)[\sin\phi + \mathrm{Bo}(\phi)]^{1/3}\,\mathrm{d}\phi\right]^{1/4} \qquad (31)$$

Thus, we can obtain the local Nusselt number from Equation 27. Next, we can also obtain the overall mean Nusselt number from Equation 28 as follows:

$$\overline{\mathrm{Nu}}(\mathrm{Ja}/\mathrm{Ra})^{1/4} = \int_0^{\phi_c}\left\{I_f(\phi)[\sin\phi + \mathrm{Bo}(\phi)]^{1/3}\,\mathrm{d}\phi\right.$$

$$\left.\times\left[2\int_0^{\phi} I_f(\phi)[\sin\phi + \mathrm{Bo}(\phi)]^{1/3}\mathrm{d}\phi\right]^{-1/4}\right\}\mathrm{d}\phi /$$

$$\int_0^{\pi} I_f(\phi)\,\mathrm{d}\phi \qquad (32)$$

Consider now the two limit cases, $e = 0$ (circular tube) and $e = 1.0$ (vertical plate). As $e = 0$, we obtain $\overline{\mathrm{Nu}}(\mathrm{Ja}/\mathrm{Ra})^{1/4} = 0.728$. Next, as $e = 1.0$, we should use $D_e = 2l/\pi$ in the above integral for a vertical plate, and then obtain $\overline{\mathrm{Nu}}_l(\mathrm{Ja}/\mathrm{Ra}_l)^{1/4} = 0.943$.

Secondly, for the cases where $F \ll 1$; i.e., the other asymptotic cases: forced-convection dominated film condensation, their critical angles ϕ_c are less than π always. We can put $F = 0$ in Equation 17 and then obtain the mean heat transfer coefficients by calculating through Equations 17–28.

Results and discussion

In this section, numerical results for the mixed-convection film condensation of downward flowing vapour on a horizontal elliptic tube are presented in two parts. In the first part, results of the condensate film thickness; i.e., flow hydrodynamics, are obtained and discussed for a wide range of F and a practical range of Bo and P. Then, the second part indicates and discusses the performance of heat transfer rates and their corresponding critical angles for the same range of parameters as the first part.

Characteristics of flow hydrodynamics: condensate film thickness δ^*; critical angle ϕ_c

Characteristics of condensate film flow hydrodynamics are illustrated in Figures 2a, and b, which are obtained from Equation 17 by employing a fourth-order Runge–Kutta integration that uses a step size of $\Delta\phi = 0.05°$. For $e = 0$ (circular tube), both the dimensionless local film thickness profile and ϕ_c coincide with Rose (1984). As e approaches unity, δ^* becomes thinner in the upper half of the elliptic tube because of the favorable pressure gradient effect $[-(\partial P/\partial x) > 0]$, while δ^* becomes thicker in the rear half of the elliptic tube because of the adverse pressure gradient effect $[-(\partial P/\partial x) < 0]$. In general, the pressure gradient caused by the effect of surface tension influences the condensate film hydrodynamics more than that caused by the vapor flow in the free-convection region (high F). In the forced-convection region (low F), the dependence of the condensate film hydrodynamics on the pressure gradient is opposite that of the free-convection region. On ϕ_c satisfying Equation 22, the rate of increase in the condensate film thickness will abruptly become extra large, and the condensate film separation will occur.

For high F or in the free-convection region, say $F = 10$ as seen in Figure 2a, the elliptic tube with higher eccentricity will drip off or separate more ahead in the rear half of the elliptic tube, because gravity force dominated. However, for low F or in the forced-convection region, say $F = 0.1$ as seen in Figure 2b, the higher the eccentricity e is, the larger the critical angle ϕ_c is; i.e., the location of the separation shifts more downstream for the elliptic tube with higher eccentricity and also better streamlined shape. According to the well-known work of Shlichting (1979), in the case of vapor flow past a circular cylinder, separation occurs at $\phi = 109.5°$ and moves downstream as the ellipse becomes more slender along the flow direction, which is just the same trend that the present work obtained for the forced–flow-dominated condensation case. However, the present flowing vapor not only passes a moving condensate liquid film but also condenses into the film. Thus, the separation point ϕ_s of vapor boundary-layer shifts more downstream than the liquid film layer ϕ_c does. If $\phi_s < \phi_c$, because of very fast vapor flow, the separation of vapor would be accompanied by a sharp pressure rise, and this could initiate an instability in the condensate film near ϕ_s. In fact, Memory and Rose (1995) observed and suggested that vapor boundary-layer separation could be suppressed under conditions of strong suction for vapor approach velocities below about 100 m/s. Furthermore, they also show that ϕ_s lies between 1.76 and 2.93 rads for a flow past circular tube in the existing earlier works. Their ϕ_ss are slightly larger than ϕ_c obtained in the present work (see Figure 2b). Generally speaking, the vapor boundary-layer separation occurring makes the prediction of heat transfer for the rear half of the tube less certain. However, because the present ϕ_c is slightly less than ϕ_s, the present work seems to be accurate and certain.

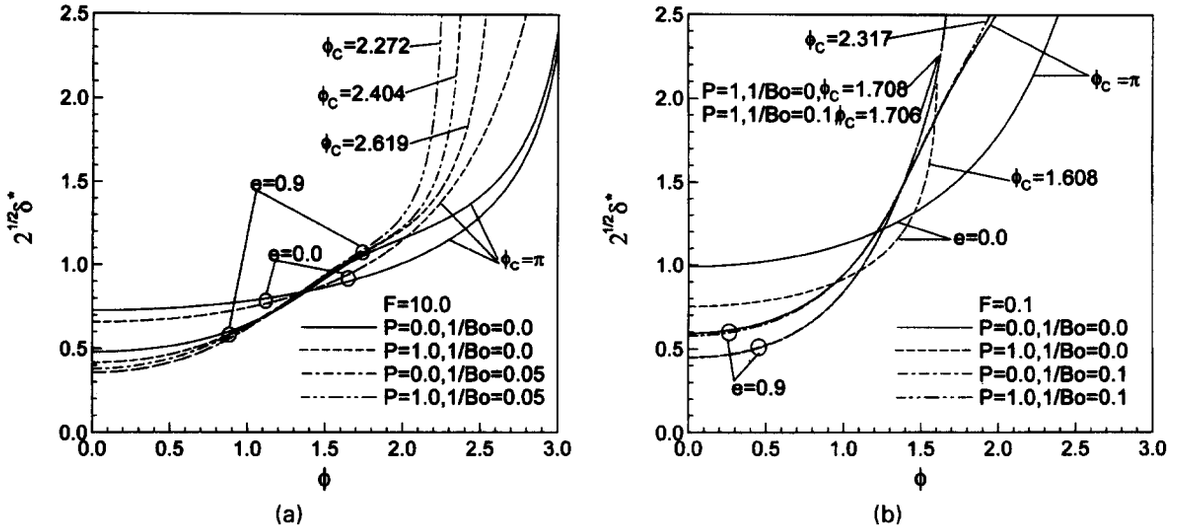

Figure 2a, b Dimensionless local film thickness around periphery of ellipse

Performance of overall mean heat transfer coefficient; critical angle ϕ_c

The overall mean heat transfer coefficients are determined from Equation 28 by numerical integrating. The step size taken is $\Delta\phi = 0.05°$. Integration with a step size twice as large produced a change in the predicted mean Nusselt number of less than 0.1%. Firstly, as $e = 0$, for two cases where $P = 0.05$ and 3.0, the present result obtained from Equation 28 is shown in Figure 3a, and compared with those of Rose (1984), Shekriladze and Gomelauri (1966), and Fujii et al. (1972). Compared with experimental data shown in Rose's (1988) work, the calculated values of $\overline{Nu}\,Re^{-1/2}$ from Rose (1984), and Fujii et al., are overpredicted; while those obtained from Shekriladze and Gomelauri without inclusion of vapor shear is underpredicted at lower bound of F. Rose (1984) takes account only of the heat transfer for the upstream half of the tube and should, therefore, be conservative. However, the present work can improve the difficulties; i.e., numerical instability arising from the zone near the critical angle, by using a very small step size of $\Delta\phi = 0.05°$, and thence, can determine the mean heat transfer up to ϕ_c. Hence, the present result agrees with the experimental data better, because the present value is adequate and lying among them in Rose's (1988) work.

As for various parametric effects upon the mean heat transfer coefficient, the discussion of the present result is illustrated as follows. The effect of vapor velocity of flow F is first discussed here. When order of F, $O(F)$ is greater than 1.0, the solutions tend to blend with the Nusselt-type condensation. For very high F or in the free-convection region, the result of Equation 28 will become the same form as that of Equation 32. Next, when $P = 0$ for a circular tube, as F decreases to zero, the value of $\overline{Nu}\,Re^{-1/2}$ gets close to "0.9," which is in accordance with Rose (1984). Furthermore, by using $l = \pi D_e/2$ in $\overline{Nu}$ and Re for the case of $e = 1.0$ (vertical plate), in the forced-convection region (low F),

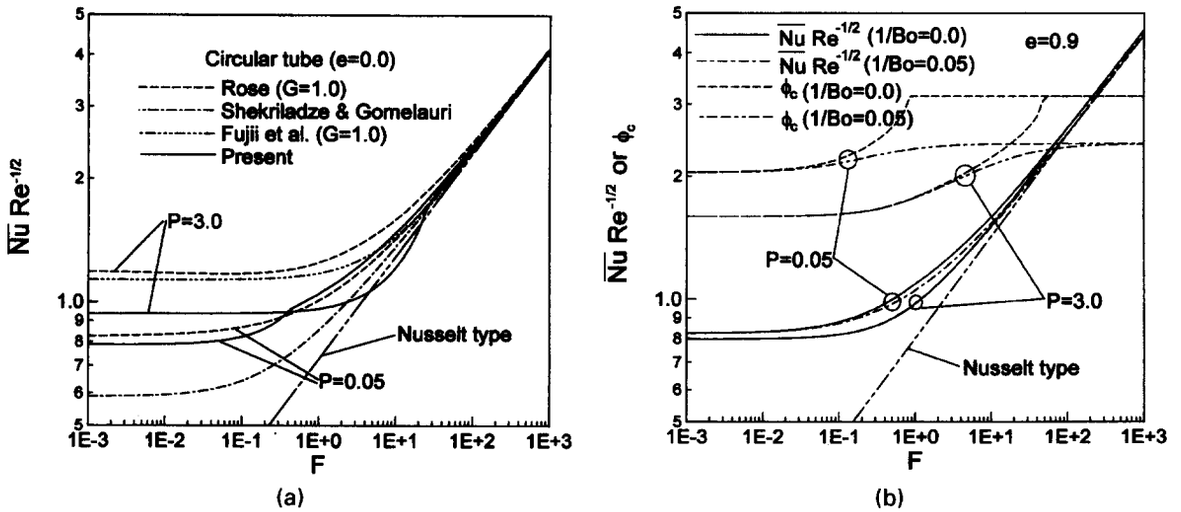

Figure 3 (a) Comparison of results of Rose (1984), Fujii et al. (1972), Shekriladze and Gomelauri (1966) and present work for mean Nusselt number. (b) Dependence of mean Nusselt number and critical angle on parameter F

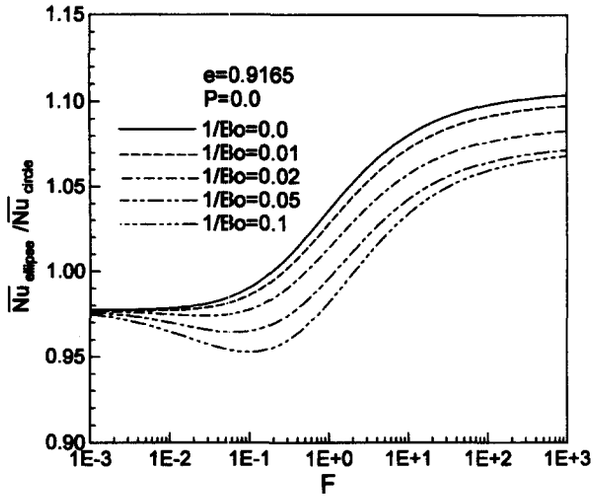

Figure 4 Effect of surface tension on mean Nusselt number at $e=0.9165$ and $P=0$

the present result also agrees well with that obtained by Shekriladze and Gomelauri (1966). But, there is a slight discrepancy between them, because the present work includes the pressure gradient term. Thus, for higher F, Shekriladze and Gomelauri underpredicts the heat transfer because of neglecting the effect of the pressure gradient. In the asymptotic case $P=0$, as F approaches zero, it is interesting to find that they both have the same result $\overline{Nu}_l Re_l^{-1/2} = 1.0$. Meanwhile, in Figure 3b, the present work extends the mean heat transfer results into an elliptic tube with $e=0.9$ and also find the same trend for ϕ_c varying and its corresponding $\overline{Nu}\,Re^{-1/2}$ varying. In other words, because ϕ_c is varying more significantly as F is decreasing or vapor velocity is increasing, the mean heat transfer coefficient is changing from the free-convection region into the forced-convection region through a transition zone. At the same time, for very high F or in the free-convection-dominated region, the present result reduces to that obtained in Yang and Chen (1993) for the free-convection film condensation.

Figure 4 shows that the effect of surface tension on the mean heat-transfer coefficient for forced and free convection at $e=0.9165$ (or $b/a=0.4$). The ordinate shows a ratio of the mean heat-transfer coefficient for the elliptic tube compared to a circular tube, based on the equal Re and condensing surface area. The inverse Bond number, 1/Bo, gives the relative effect of surface tension to inertia, and is typically about 0.02 for steam and 0.002 for refrigerants. For refrigerants, the effect of surface tension on the mean heat-transfer coefficient is almost negligible. Moreover, it is obvious that these influences are more significant in the free-convection region (or high F), where an increase in 1/Bo leads to a small decrease (by within 4%) in the mean heat transfer for an ellipse. Because of the increasing severity of surface curvature at the very top and bottom of the elliptic tube, as eccentricity increases, the discrepancy between elliptic tube and circular tube is accentuated. In the forced-convection region (or low F), the influence of surface tension on the mean heat transfer coefficient is much smaller (negligible), because any thinning of the film is dominated by interfacial vapor shear effects.

As for the effect of pressure gradient on the mean heat-transfer coefficient and the critical angle, we can see that, in Figures 5a and b, during $\phi_c=\pi$, P does not affect the value of $\overline{Nu}\,(Re)^{-1/2}$. In other words, the mean heat transfer coefficient remains unchanged as P increases, until $\phi_c<\pi$ occurs. This is caused by the third term involving P in Equation 17; i.e., the pressure gradient term attributable to potential flow has a weighted factor "$\sin 2\phi$," hence, it automatically vanishes after being integrated over the whole tube. Furthermore, for each case of F, ϕ_c will begin to decrease at some particular value of P, and this decrease in ϕ_c makes the corresponding $\overline{Nu}\,Re^{1/2}$ start to decrease and then turn up. In the practical ranges of P, such as $P<1$ for refrigerants and $P<0.1$ for steam, the pressure gradient effect usually makes a small (negligible) decrease in the mean heat transfer coefficients, because ϕ_c is reduced by the effect of pressure gradient.

Figures 6a and b show that the dependence of mean Nusselt number and critical angle on eccentricity. Firstly, in Figure 6a, for $F=10$, we can see that, as e increases up to 0.999 (nearly 1.0), $\overline{Nu}\,Re^{1/2}$ increases up to 10.89% for $P=0$ and $1/Bo=0$; 12.29% for $P=0$ and $1/Bo=0.05$; 14.11% for $P=1.0$ and $1/Bo=0$; and 15.92% for $P=1.0$ and $1/Bo=0.05$. Next, in Figure 6b, for $F=0.1$ (forced convection), we can also see that, as e is increasing up to 0.999, $\overline{Nu}\,Re^{-1/2}$ decreases up to 6.32% for $P=0$ and $1/Bo=0$; and 8.24% for $P=0$ and $1/Bo=0.1$; but $\overline{Nu}\,Re^{-1/2}$ increases up to 11.08% for $P=0.1$ and $1/Bo=0$;

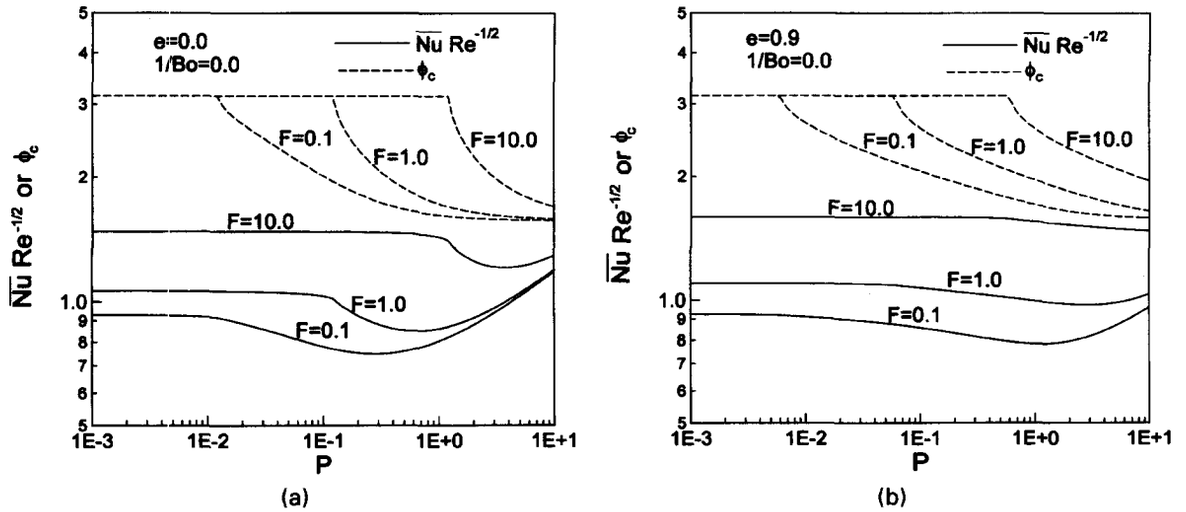

Figure 5a, b Dependence of mean Nusselt number and critical angle on parameter P

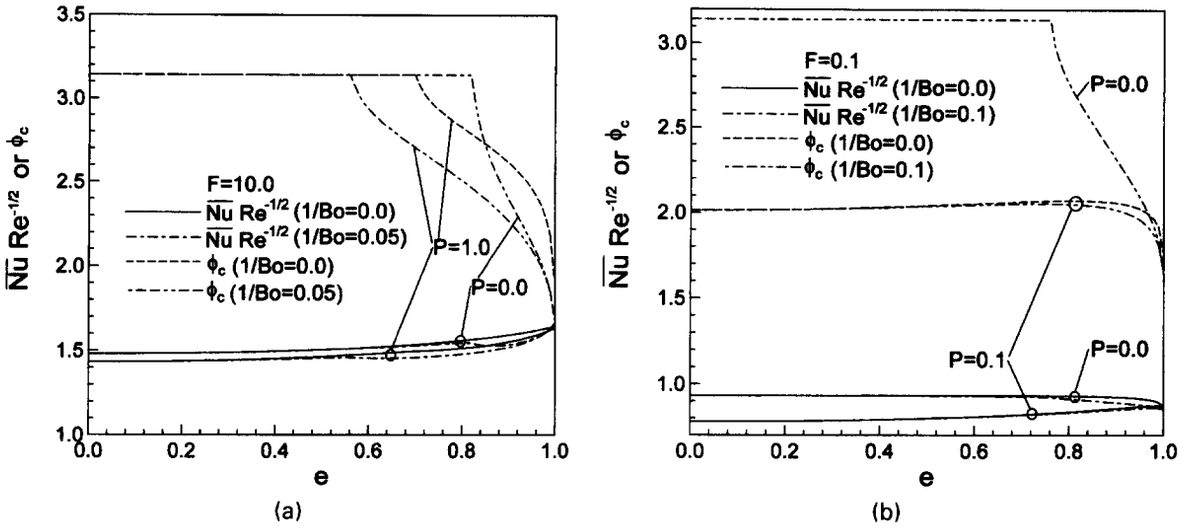

Figure 6a, b Dependence of mean Nusselt number and critical angle on eccentricity

and 9.55% for $P = 0.1$ and $1/Bo = 0.1$. The reason for enhancement of the mean heat transfer for elliptic tubes, when $P = 0.1$, is caused by an increase in ϕ_c or a delay in film boundary-layer separation that occurs with the better streamlined body as e is higher up to practical limit $e = 0.95$ ($b/a = 0.3$). Furthermore, for no pressure gradient inclusion ($P = 0$), its ϕ_c starts to decrease at some particular value of e in the forced-convection region, hence, the mean heat transfer coefficient starts to decrease at that e, as e is increasing.

Conclusions

(1) The model given by Equation 17 is the result of extending and merging several extant techniques for combined free- and forced-convection film condensation, including both a circular tube and flat plate.

(2) Pressure gradient caused by potential flow and surface tension effects on the mean heat-transfer coefficients are small. For low F (forced convection), the effect of surface tension on the mean heat transfer is almost negligible.

(3) The practical values of e are 0.8–0.95 around (b/a: 0.3–0.6), compared to a circular tube with the equal condensing surface area, the mean heat transfer is enhanced up to about 16% for high F and about 11% for low F, under inclusion of pressure gradient effects attributable to both potential flow and surface tension

(4) Although the present results for both circular tube and vertical plate have been confirmed by earlier experimental works, experimental verification of these predicted trends for elliptic tubes must be carried out by future researchers.

References

Adams, V. H., Marto, P. J. and Memory, S. B. 1993. Free- and forced-convection laminar film condensation on a horizontal elliptical tube. In *Condensation and Condenser Design*, 1st ed. ASME, New York, 417–429

Blangetti, F. and Naushahi, M. K. 1980. Influence of mass transfer on the momentum transfer in condensation and evaporation phenomena. *Int. J. Heat Mass Transfer*, **23**, 1694–1695

Churchill, S. W. 1986. Laminar film condensation. *Int. J. Heat Mass. Transfer*, **29**, 1219–1226

Fujii, T., Uehara, H. and Kruata, C. 1972. Laminar film condensation of flowing vapor on a horizontal cylinder. *Int. J. Heat Mass Transfer*, **15**, 235–246

Jacobi, A. M. 1992. Filmwise condensation from a flowing vapor onto isothermal, axisymmetric bodies. *J. Thermophys. Heat Transfer*, **6**, 321–325

Karimi, A. 1977. Laminar film condensation on helical reflux condensers and related configurations. *Int. J. Heat Mass Transfer*, **20**, 1137–1144

Krupiczka, R. 1985. Effect of surface tension on laminar film condensation on a horizontal cylinder. *Chem. Eng. Process*, **19**, 199–203

Memory, S. B. and Rose, J. W. 1995. Forced-convection film condensation on a horizontal tube—Influence of vapor boundary-layer separation. *J. Heat Transfer*, **117**, 529–533

Nusselt, W. 1916. Die oberflachen kondensation des wasserdampfes. *Zeitsehrift des Vereines Deutscher Ingenieure*, **60**, 541–546; 569–575

Panday, P. K. 1987. Laminar film condensation of downward flowing vapor on a horizontal elliptical cylinder—Numerical solutions. *Int. Comm. Heat Mass Transfer*, **14**, 33–43

Rohsenow, W. M. 1956. Heat transfer and temperature distribution in laminar film condensation. *Trans. ASME*, **78**, 1645–1648

Rose, J. W. 1984. Effect of pressure gradient in forced convection film condensation on a horizontal tube. *Int. J. Heat Mass Transfer*, **27**, 39–47

Rose, J. W. 1988. Fundamentals of condensation heat transfer: Laminar film condensation. *JSME Int. J. Series II*, **31**, 357–375

Shekriladze, I. G. and Gomelauri, V. I. 1966. The theoretical study of laminar film condensation of a flowing vapor. *Int. J. Heat Mass Transfer* **9**, 581–591

Schlichting, H. 1979. Flow past a circular cylinder. In *Boundary Layer Theory*, 7th ed., McGraw-Hill, New York, 215–218

Sparrow, E. M. and Gregg, J. L. 1959. Laminar condensation heat transfer on a horizontal cylinder. *J. Heat Transfer*, **81**, 291–296

Yang, S. A. and Chen, C. K. 1993. Role of surface tension and ellipticity in laminar film condensation on a horizontal elliptical tube. *Int. J. Heat Mass Transfer*, **36**, 3135–3141